European Journal of Agronomy 150 (2023) 126955

Contents lists available at ScienceDirect

European Journal of Agronomy

journal homepage: www.elsevier.com/locate/eja

Combining functional physiological phenotyping and simulation model to estimate dynamic water use efficiency and infer transpiration sensitivity traits

Ting Sun [a,1], Rui Cheng [b,1], Rujia Jiang [a], Yunxiu Liu [a], Yudong Sun [b], Zhuoyi Wang [a], Pingping Fang [a], Xinyang Wu [a], Kang Ning [a], Pei Xu [a,*]

[a] Key Laboratory of Specialty Agri-product Quality and Hazard Controlling Technology of Zhejiang Province, College of Life Sciences, China Jiliang University, Hangzhou 310018, PR China

[b] Vegetable Research Centre, Huaiyin Institute of Agricultural Sciences of Xuhuai Region in Jiangsu, Huaian 223001, PR China

ARTICLE INFO

Keywords:
Phenotyping
Transpiration model
Water use efficiency
Sensitivity
Ideotype
Drought

ABSTRACT

With agricultural drought increasingly prevalent worldwide, it's essential to enhance crop productivity while minimizing water consumption for sustainable production. Yield performance depends on the interplay between plant transpiration rate (TR) and water use efficiency (WUE), but balancing the two in breeding programs is challenging due to our incomplete understanding of these traits. In this study, we introduce a method for estimating genotype-specific traits that reflect the sensitivity of TR to solar radiation ($S_{TR\text{-}Rad}$) and vapor pressure deficit ($S_{TR\text{-}VPD}$), by combining state-of-the-art functional physiological phenotyping (FPP) and TR model. Genotypic difference of $S_{TR\text{-}Rad}$ and $S_{TR\text{-}VPD}$ in three watermelon accessions, and their quantitative impacts on dynamic WUE patterns were dissected under evolving developmental stage and water availability. We also demonstrate the feasibility and effectiveness of calculating dynamic WUE and biomass production using WUE model. By combining the TR model and WUE model, a general principle for TR ideotype design is proposed, which highlights the benefits of lowering $S_{TR\text{-}VPD}$ to increase WUE and increasing $S_{TR\text{-}Rad}$ to offset the decline of TR. FPP-enabled phenotypic selection will help screen for elite crops lines with desired TR sensitivities.

1. Introduction

Global farming land area subject to drought is increasing due to the enhanced evapotranspiration associated with increased temperature, net radiation and decreased relative humidity (IPCC, 2021). Improving crop productivity, particularly under deficit water condition, is essential to safeguard food security under the context of global climate change. Stomata is the gateway of both water efflux (transpiration) and CO_2 intake (assimilation). The plant transpiration rate (TR) and the ratio of CO_2 assimilation to TR, which is known as water use efficiency (WUE), collectively determine biomass production and yield (Steduto et al., 2012; Vadez et al., 2014). Large efforts are being devoted to developing drought-resistant crops by adopting a strategy of restricting stomatal closure and thereby water loss; however, a tradeoff between increased WUE and decreased TR as a consequence of stomatal restraint has long impeded breeding for agronomically useful varieties (Dalal et al., 2019). In the past, the isotope method was commonly used to select crop varieties with high WUE, but such varieties typically possess smaller leaf area index (LAI), shorter growth periods, lower TR, and lower biomass production. Despite exhibiting enhanced water-use efficiency, these cultivars usually fail to achieve satisfactory yields (Blum, 2005, 2009). In order to develop plant varieties that balance water-saving and high-yield, it is imperative to have a comprehensive understanding of the interrelationships among WUE, TR, and yield.

WUE has conventionally been regarded as a conservative parameter that is species or cultivar-specific. However, gas exchange measurements at the leaf or canopy level have revealed that WUE is a highly dynamic variable, exhibiting changes even within the same plant at different times of the day and on different days (Nelson et al., 2018; Peddinti et al., 2019; Yang et al., 2021). WUE typically peaks in the morning, followed by a gradual decrease to a low steady-state, and a slight recovery after sunset (Fracasso et al., 2017; Jhou et al., 2017). This

* Corresponding author.
E-mail address: peixu@cjlu.edu.cn (P. Xu).
[1] Equal contribution.

https://doi.org/10.1016/j.eja.2023.126955
Received 23 January 2023; Received in revised form 27 August 2023; Accepted 27 August 2023
Available online 31 August 2023

daily pattern is mainly attributed to WUE's strong dependence on VPD at smaller time scales (Song et al., 2017). Theoretically, it is feasible to improve the daily WUE and biomass production of crops by altering the daily trend of TR, specifically by increasing TR during high-WUE hours and decreasing it during low-WUE hours, without changing the total daily TR (Ghanem et al., 2020; Vadez et al., 2014).

Identifying the factors that affect TR can have a substantial impact on regulating diurnal TR pattern and improving WUE. TR is a complex traits that is not only governed by internal factors such as LAI and structure (e.g. cuticle thickness, stomata number), but also by external factors such as temperature, relative humidity, light intensity, wind speed and soil water availability (Kubota, 2020). VPD and solar radiation (Rad) are the primary driving factors among the environmental factors that affect TR (Oogathoo et al., 2020). According to Pieruschka et al. (2010), TR is mainly controlled by the diffusion gradient of water vapor inside and outside the stoma driven by VPD, and internal evaporation driven by latent heat from Rad. Since the diurnal patterns of VPD and Rad are inconsistent (Gosa et al., 2019), the sensitivities of TR to VPD and Rad would have a strong impact on the dynamic TR profile.

The soil-plant-atmosphere continuum (SPAC) is a complex system in which environmental factors, TR and WUE interact with each other. Both VPD and Rad drive and influence the diurnal patterns of TR, with VPD affecting the daily variation in WUE, and the diurnal changes in TR affecting the daily-scale WUE. Nevertheless, ascertaining the interrelationships between these variables and their influence on final biomass production poses a significant challenge. Models, ranging from simple empirical formulas to complex ecophysiological models involving multiple variables and interactions, offer a powerful tool for quantifying these interactions (Génard et al., 2016). Several types of TR models have been established, such as the Penman-Monteith equation, Jarvis model, and Ball-Berry model (Katsoulas et al., 2019). Synthetic models that combine TR and photosynthesis models are also employed to estimate WUE (Yu et al., 2001; Yu et al., 2004).

In recent years, the emerging technique of functional physiological phenotyping (FPP) has presented groundbreaking opportunities for the phenotyping of plant water relations (Chenu et al., 2018; Halperin et al., 2017; Li et al., 2020; Xu et al., 2015). The Plantarray platform exemplifies a non-destructive and high-throughput tool that allows for high-resolution (every 3 min) and continuous recording of meteorological variables, including photosynthetically active radiation (PAR), VPD, and soil volumetric water content (VWC), as well as physiological traits such as diurnal TR, daily TR, and biomass gain, based on the lysimeter principle (Dalal et al., 2020; Halperin et al., 2017). In this study, we aimed to combine the physiological phenotypic data obtained from the Plantarray platform and TR model to quantify the traits of TR sensitivity to variations in environmental Rad and VPD in different ecotypes of watermelon. Moreover, an effective approach depending on WUE model (Sinclair et al., 2020) is proposed to estimate dynamic WUE, a traditionally challenging trait to measure, based on TR and VPD. Additionally, we investigate the impact of TR sensitivity to Rad and VPD on daily WUE and biomass, and the implications for TR ideotype design are discussed. This study demonstrates the great promise of leveraging advanced phenotyping techniques and existing modeling methods to tackle the long-standing complex trait challenge.

2. Materials and methods

2.1. Plant materials and cultivation

The study was conducted during the spring and summer seasons of 2021 in Huai'an (33.62°N, 119.02°E), Jiangsu province, China. Our study utilized watermelon as the research object, owing to its developed vascular system and abundant daily water flow. Three genotypes of watermelon, i.e., a wild watermelon accession "PI-296341-FR" (*Citrullus lanatus* var. citroides), a cultivated watermelon variety "Jincheng No. 5″ (*Citrullus lanatus* var. lanatus, hereafter "JC5″) popular in Northwest China, and a drought-tolerant inbred line of *Citrullus lanatus* var. lanatus "HA" were used in this study. The watermelon seeds were disinfected by being exposed to 65 °C water for 30 min. After treatment, the seeds were wrapped in moist towels and incubated at a constant temperature of 30 °C until white shoots appeared. For each accession, 10 plump seeds were sowed in 32 cell trays filled with Blond Gold substrate (Pindstrup Mosebrug A/S, Denmark) and covered with a layer of vermiculite. The seedlings were irrigated with a nutrient solution of "Zhonghua Yangtian" series (Sinofert, China) at a concentration of 1/500 when the soil was slightly moist. One seedling at the three-leaf stage was transplanted per pot (16 cm × 13 cm×18 cm, 1.5 L) with a kiln-fired porous ceramic from a unique mineral deposit in Mississippi, known as Profile Porous Ceramic substrate (Profile Products LLC, USA; diameter: 0.2 mm, pH: 5.5 ± 1, porosity: 74, and CEC: 33.6 mEq/100 g). Using the gravimetric method, we measured the field capacity of the PPC substrate employed in potted plants, and the average value obtained was 54.9% after assessing the moisture content through pre- and post-drying weight measurements.

2.2. Experimental design

The phenotyping was conducted using Plantarray (Plant-DiTech, Israel, Fig. 1). Plantarray is a high-throughput physiological phenotyping gravimetric platform that includes a gravimetric system, soil and atmospheric probes, a controller, and irrigation valves (Dalal et al., 2020; Halperin et al., 2017). This system provides a simultaneous measurement and detailed physiological response profile for plants in each pot. To ensure a stable testing environment, the Plantarray platform was placed in a glass greenhouse that measures 10 m × 5 m × 4 m (length × width × height). The greenhouse's top is made of 4 mm tempered glass, while the surrounding and partition walls use 4 mm float glass with a light transmittance of over 87%. Additionally, the greenhouse features auxiliary systems such as heating, circulation, ventilation, and shading. The ground source heat pump was triggered when the temperature drops below 20 ℃, and the cooling system was activated when the temperature exceeds 35 ℃. Fig. 1c-e illustrate the natural daily variation patterns of the environment.

During the 5-leaf stage, four replicates for each genotype were transferred to the load cell of Plantarray following a completely randomized design. To prevent soil water evaporation, the pot surface was wrapped with plastic film. The irrigation nozzle and the soil sensor 5TM were inserted into the soil, with cares to avoid hurting the main roots of the plants. Water and nutrient supplements (Yamazaki nutrient solution) were controlled by the automatic irrigation system of Plantarray. Experiment in each growth season included three treatment periods, i.e., well-irrigation (WI), progressive water deficit (WD) and water recovery (W*R*). Under the WI and W*R* phase, nutrient solution was provided by irrigation for 240 s (oversaturated) at 23:00, 1:00, 2:00, and 3:00 of a day, respectively, and no nutrient solution was supplied during the WD stage. In this study, all three watermelon varieties displayed noticeable leaf wilting on April 5th (spring season) and June 27th (summer season). The specific VWC values for PI296341-FR, JC, and HA were 0.095, 0.088, and 0.090 in the spring season, and 0.095, 0.096, and 0.102 in the summer season, respectively. When the VWC reached a level of 0.05, the plants displayed severe wilting, accompanied by a significant reduction in the whole-plant transpiration rate, nearly reaching zero. However, after rehydration, rapid recovery was observed, suggesting that the VWC threshold for irreversible wilting was below 0.05.

2.3. Functional physiological phenotyping datasets

The Plantarray system is a weighing type lysimeter that consists of highly sensitive, temperature compensated load cells (Halperin et al., 2017). A series of functional physiological traits relative to the water loss by plant transpiration and plant growth could be obtained by the weight change throughout the day using the SPAC software

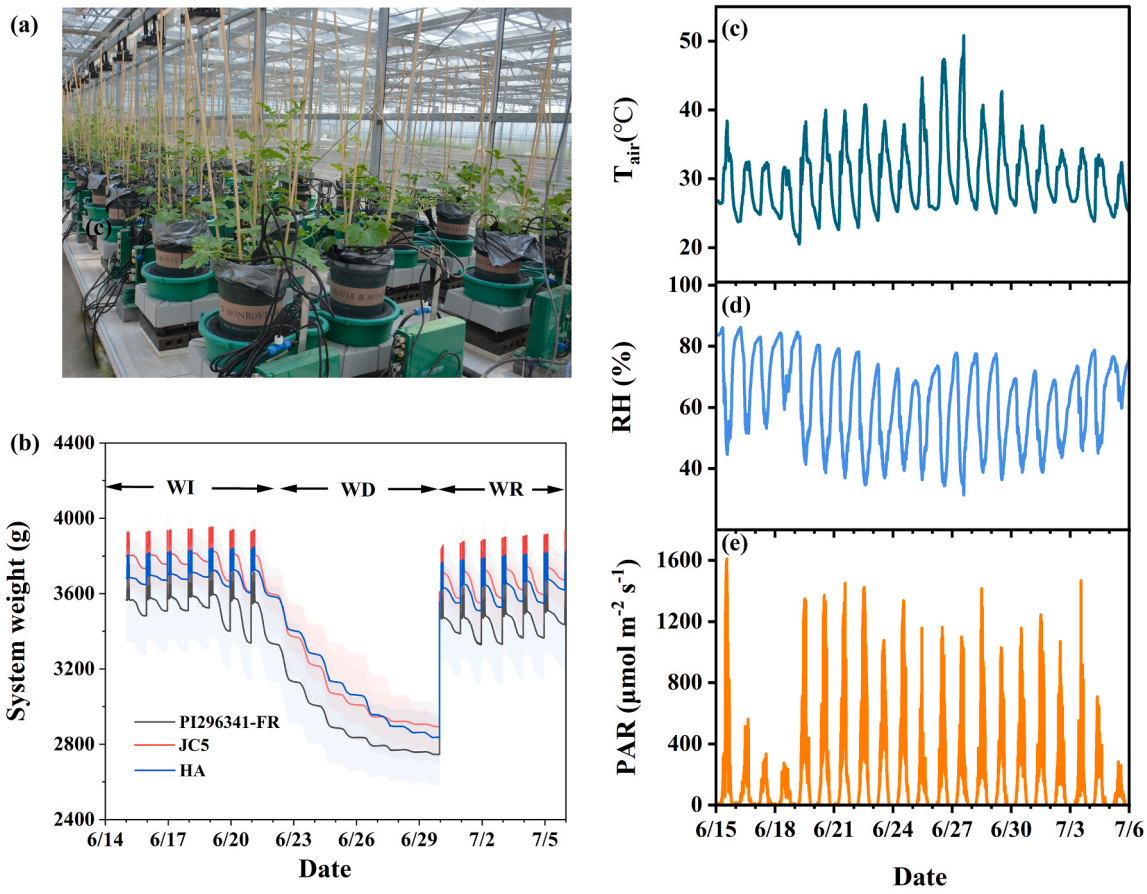

Fig. 1. Parameters of soil–plant–atmosphere continuum monitored by "Plantarray" phenotyping platform. a, overview of the automated physiological phenotyping array loaded with watermelon seedlings. b, system weights that were recorded every 3 min during the experimental course. Shadow areas show the observed variation. The experiment was divided into the well-irrigation (WI), progressive water deficit (WD), and water recovery (W*R*) phases. c-e, meteorological parameters, i.e., air temperature (T_{air}, ℃, c), relative humidity (RH, %, d), and photosynthetic active radiation (PAR, μmol m^{-2} s^{-1}, e) during the summer-season experiment in 2021.

implemented in the Plantarray system (https://spac.plant-ditech.com). Briefly, the pre-dawn system weight (averaged over 4:00–4:30 a.m.) was recoded as W_m at the end of the free drainage after saturated irrigation, and system weight in the evening (averaged over 9:00–9:30 p.m.) was recoded as W_e before irrigation, both of which were stable due to no water loss by plant transpiration and water input from irrigation during this period. As each pot on the system was covered with plastic film, soil evapotranspiration was prevented. The whole-plant daily transpiration (*E*, g d^{-1}) was calculated as the difference between the W_m and W_e for each day. To calculate the daily plant growth (*PG*, g FW d^{-1}), the W_m values of consecutive days were subtracted. This algorithm is based on the principle that the weight of the substrate from different days should theoretically remain consistent after excess water is drained out through saturated irrigation (field capacity). As a result, any differences in system weight are attributed to plant growth (Halperin et al., 2017). The whole-plant WUE during the well irrigation period was thus determined by the ratio between the accumulated *PG* and *E*. The momentary whole-plant transpiration (TR, g min^{-1}) at 3-min step was calculated by multiplying the first derivative of the measured load-cell time series by − 1, assuming that the plant's weight gain during the short time interval used to calculate the TR was negligible (Halperin et al., 2017).

The air temperature (T_{air}, ℃) and relative humidity (RH, %), photosynthetically active radiation (PAR, μmol m^{-2} s^{-1}) above the canopy, and soil volumetric water content (VWC, m^3 m^{-3}) in each pot were measured by the VP-4, PYR solar radiation sensor, and 5TM (Decagon Devices, Pullman, Wash, USA), respectively (Fig. 1c-e, Fig. S1). VPD (kPa) was calculated according to Halperin et al. (2017).

2.4. Simulation study

2.4.1. TR model

We choose the simulation models which account for the response of TR to the major meteorological variables and plant growth, following the principle that model obtains simple structure using as few parameters as possible. A modified Penman–Monteith model which is appropriate for greenhouse environment, is employed to simulate the TR of watermelons in this study, which has been test for cucumber and tomato plants (Jo et al., 2021; Medrano et al., 2005). The diurnal TR could be described as a function of radiation, VPD and leaf area index (LAI):

$$\lambda TR_i = S_{TR-Rad}\left(1 - e^{-KLAI_d}\right)Rad_i + S_{TR-VPD}LAI_d * VPD_i \quad (1)$$

where λ is the vaporization heat of water (J kg^{-1}), TR_i is the instantaneous TR, *K* is the light extinction coefficient (0.86), Rad_i is the instantaneous solar radiation (W m^{-2}, converted from PAR), LAI_d is the daily leaf area index (m^{-2} m^{-2}). VPD_i is the instantaneous vapor pressure deficit. S_{TR-Rad} and S_{TR-VPD} represent the sensitivity of TR to changes in Rad and VPD, respectively.

The LAI was estimated based on *E* in each experiment unit by considering the individual difference, as follows (Fig. 2a):

Step 1, dynamic TR recorded in a frequency of every 3 min across a day was fitted to the observed radiation and VPD, thus optimum S_{TR-Rad}, S_{TR-VPD}, and LAI in the modified Penman–Monteith equation (Eq. 1) were estimated according to nonlinear least square (NLS) method and trust-region algorithm. Only daily LAI with robust goodness of fit

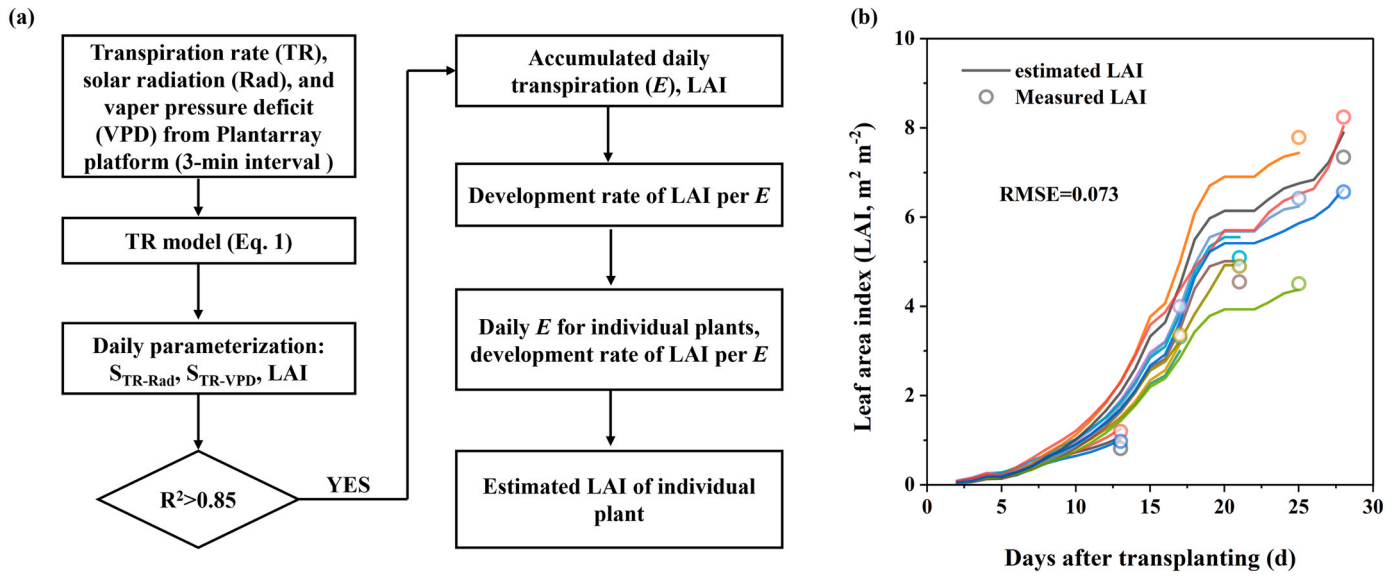

Fig. 2. Flow chart for estimating leaf area index (LAI) and the comparison of estimated and measured LAI. Daily estimated LAI of watermelon plant in individual experiment unit of Plantarray was shown as multi colored lines until destructive sampling, according to the methods described in the Section 2.4.1. At 13,17, 21, 25 and 28 days after transplanting, leaf tissues from 3 experiment units were collected from the watermelon plants and the leaf areas (circles) were measured using a LA-S leaf area analyzer system. RMSE represents root mean square error.

(adjusted R^2 >0.85) were picked for subsequent calculations. Step 2, we checked the accumulated *E* measured by Plantarray and the estimated LAI from daily fitting of step 1, where good linear relationship was found between them. Therefore, a constant LAI increase rate per *E* was estimated for individual experiment units (Fig. S2), and then daily values of LAI of individual experiment units were re-calculated according to daily measured *E* and estimated LAI increase rate per *E*.

Daily S_{TR-Rad} and S_{TR-VPD} were then determined with observed TR, Rad, VPD and re-calculated LAI during Step 2 for WI, WS, and W*R* stages, respectively. The parameter fitting was carried out using the trial version of MATLAB 2018b (MathWorks, Inc., USA), where the goodness of fit was assessed.

2.4.2. WUE model

The initial definition of WUE considers the resistances to diffusion resulting from stomata, leaf aerodynamic boundary layer, and leaf mesophyll resistance, and can be ultimately simplified to:

$$\mathrm{WUE} = \frac{K_\mathrm{d}}{\mathrm{VPD_d}} \tag{2}$$

where $\mathrm{VPD_d}$ is the mean VPD over a day. K_d is a species-specific coefficient that reflects the CO_2 concentration in the stomatal chamber, which has been validated as among different crops (Sinclair et al., 1984; Tanner and Sinclair, 1983). K_d was estimated as 6.5 kPa in this study for watermelon plant with the data of FPP and WUE (g DW g^{-1} H_2O) obtained from destructive sampling during a long growth period.

To estimate WUE over a long period, VPD needs to be integrated over a growth season and weighted by the TR over the course (Ghanem et al., 2020; Vadez et al., 2014). Applying the same logic to a single day, Sinclair and Vadez (2012) proposed an assumption that the weighting of this component based on the TR throughout the day leads to the possibility of obtaining altered values if there are genotypic variations in the TR profile throughout the day. Therefore, during a computation interval (i), the mean VPD ($\mathrm{VPD_i}$) is weighted for the mean TR ($\mathrm{Tr_i}$) to calculate the estimated WUE ($\mathrm{WUE_e}$) as in the following integrating equation:

$$\mathrm{WUE_e} = \frac{\int \frac{K_\mathrm{d}\mathrm{Tr_i}}{\mathrm{VPD_i}}}{\int \mathrm{Tr_i}} \tag{3}$$

And biomass gain during this period could be estimated as:

$$\mathrm{Biomass_e} = \frac{\int K_\mathrm{d}\mathrm{Tr_i}}{\mathrm{VPD_i}} \tag{4}$$

2.4.3. Model calibration and validation

Independent experiment was conducted to verify the approach of LAI estimation in TR model, where estimated LAI was compared to the LAI measured by an LA-S leaf area analyzer system (Wanshen Technology Co., Hangzhou, China). WUE model were validated using the datasets of gas exchange parameters measured by the canopy photosynthesis and transpiration system (CAPTS 100, Shanghai Millet Hill Biotech Co., Ltd., China) from wheat plants cultivated in the field in 2021, because the Plantarray system does not directly measure photosynthesis data. The gas exchange parameters of the 1 m × 1 m canopies were measured automatically every 30 min using CAPTS 100 consisting of a cubic transparent chamber, which can be open and closed automatically with programming and equipped with CO_2, humidity, air pressure, and temperature sensors in it (Song et al., 2016). Canopy gas exchange rate was measured according to the change rate of CO_2 and H_2O concentrations in the chamber during the closure of the chamber under uncontrolled conditions. The parameter K_d for wheat plants in this study was estimated using the least square method by fitting the estimated and measured daily WUE obtained during the growth period of March; then estimated and measured WUE at half-hour intervals and daily intervals during the days between April 5 and April 10 of 2021 were shown in Fig. S3.

We used the root mean square error (RMSE) and coefficient of determination (R^2) as measures for fitness between estimated and observed values to quantify the model performance:

$$\mathrm{RMSE} = \sqrt{\frac{1}{\mathrm{n}}\sum_{i=1}^{n}(y_i - \hat{y}_i)^2} \tag{5}$$

$$R^2 = \frac{\sum_{i=1}^{n}[(y_i - \overline{y_i}) \times (\hat{y}_i - \overline{\hat{y}_i})]}{\sqrt{\left[\sum_{i=1}^{n}(y_i - \overline{y_i})^2 \times \sum_{i=1}^{n}(\hat{y}_i - \overline{\hat{y}_i})^2\right]}} \tag{6}$$

where y_i is the observed value, $\hat{y}_i$ is the corresponding simulated value,

and n is the total number of observations or simulations, $\bar{y}$ and $\bar{\hat{y}_i}$ are mean values for y_i and $\hat{y}_i$, respectively.

2.4.4. Transpiration ideotype design

We conducted simulations with the inputs of 5-day meteorological data from each of the WI and WD phases and the artificial combinations of $S_{TR\text{-}Rad}$ and $S_{TR\text{-}VPD}$ extremes (i.e., highest $S_{TR\text{-}Rad}$ × lowest $S_{TR\text{-}VPD}$, lowest $S_{TR\text{-}Rad}$ × lowest $S_{TR\text{-}VPD}$, highest $S_{TR\text{-}Rad}$ × highest $S_{TR\text{-}VPD}$, and lowest $S_{TR\text{-}Rad}$ × highest $S_{TR\text{-}VPD}$ in the model) adopted from the 3 watermelon accessions averaged over each 5-day course. Our primary objective was to examine the effects of the $S_{TR\text{-}Rad}$ and $S_{TR\text{-}VPD}$ combinations on TR, WUE, and biomass production. For this purpose, a standardized LAI value of 3 that approximates the mean value of three watermelon accessions was used, to eliminate the effect of canopy size in the simulations.

2.5. Statistical analysis

Two-way analysis of variance (ANOVA) was conducted on $S_{TR\text{-}Rad}$ and $S_{TR\text{-}VPD}$, considering both distinct days and genotypes as factors for WI, WD and W*R* phases, respectively. Multiple comparisons between genotypes were performed using the least significant difference (LSD) method. Statistical analysis and graphical presentation were performed using the student version of Origin 2022 software (OriginLab Corporation, USA).

3. Results

3.1. Quantification of TR sensitivity to Rad and VPD

In this study, TR, Rad, and VPD of various plant species were measured at a 3-min frequency using the Plantarray platform. Accurate estimation of LAI is crucial for the precise identification of the component traits of TR, $S_{TR\text{-}Rad}$ and $S_{TR\text{-}VPD}$, according to Eq. 1. The validity of the LAI estimation method described in Section 2.4.1 was confirmed by using independent data. Fig. 2b illustrates the change in estimated LAI over time until destructive sampling, which is comparable to the LAI value measured by the LA-S leaf area analyzer, with a low root mean square error (RMSE) of 0.073. Subsequently, daily $S_{TR\text{-}Rad}$ and $S_{TR\text{-}VPD}$ were estimated by fitting the TR to measured Rad, VPD and estimated LAI. The fitted TR dynamics well reproduced the measured diurnal TR, as evidenced by the high correlation (R^2 =0.94) between them and the low total RMSE of only 0.05 g min^{-1}, taking the commercial cultivar "JC5″ for example (Fig. 3a). In the fitting of PI296341-FR and HA, there was also a demonstration of high R^2 (0.92 and 0.91) and low RMSE (0.06 g min^{-1} and 0.08 g min^{-1}). We performed a two-way ANOVA to evaluate the impact of both genotypes and different days on daily $S_{TR\text{-}Rad}$ and $S_{TR\text{-}VPD}$, during each phase of WI, WD and W*R*. The analysis revealed

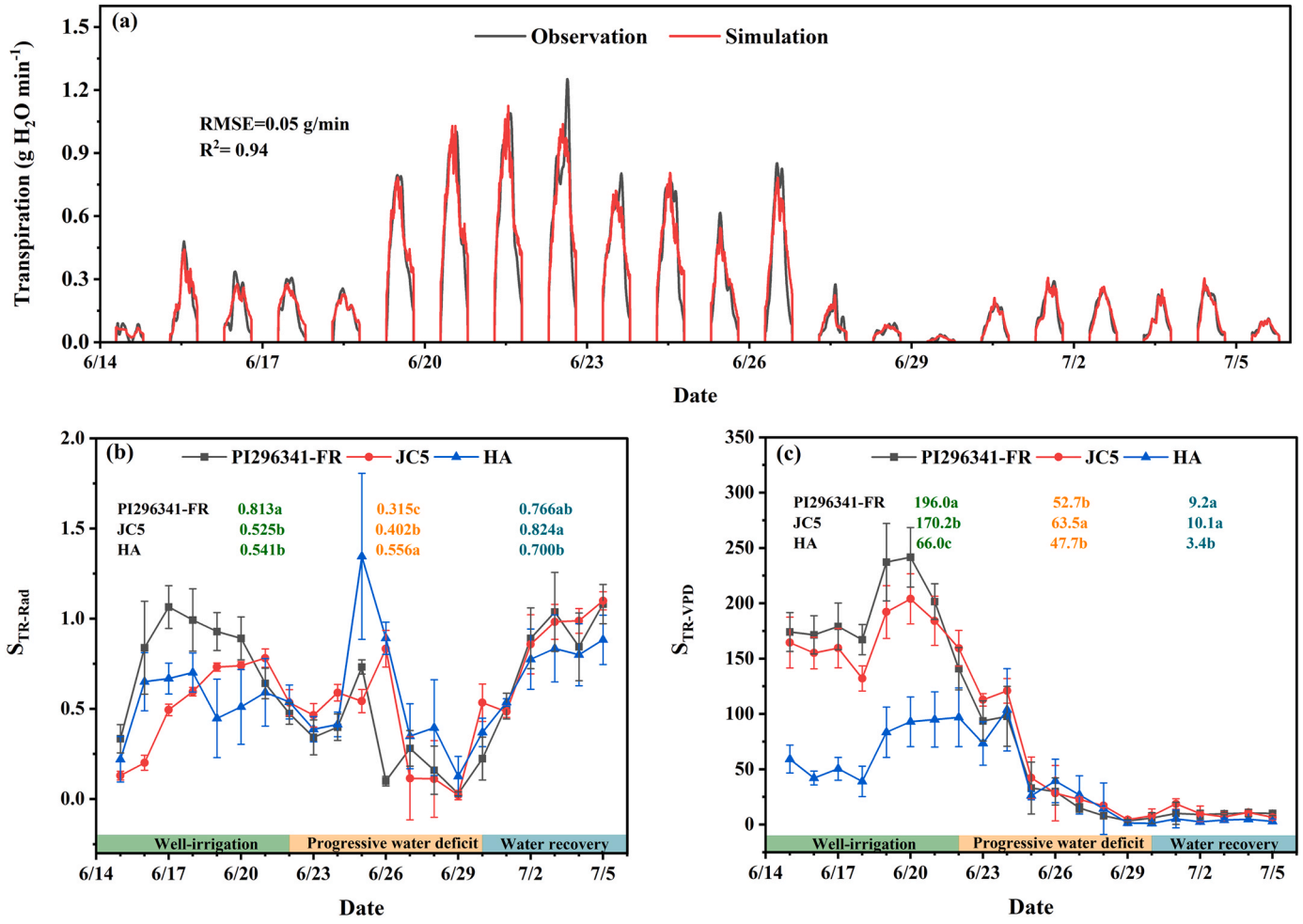

Fig. 3. Simulation of diurnal transpiration by using the modified Penman-Monteith model (Eq. 1). a, observed and simulated diurnal variation of transpiration rate during summer-season experiment in 2021, taking an experiment unit of JC5 for instance. The observations and simulations were both by a 3-min step. b-c, fitted daily $S_{TR\text{-}Rad}$ (b) and $S_{TR\text{-}VPD}$ (c) for Eq. 1. Multiple comparison results among three genotypes (PI296341-FR, JC5, and HA) were shown as mean values with lowercase letters to show statistically significant differences for the well-irrigation (WI), progressive water deficit (WD) and water recovery (W*R*) phases, respectively.

significant genotypic variation and substantial change in both $S_{TR\text{-}Rad}$ and $S_{TR\text{-}VPD}$ across the treatment phases ($P < 0.01$, Fig. 3b, c, Fig. S4). In general, $S_{TR\text{-}Rad}$ decreased as the water deficit progressed and rapidly recovered when water was resumed (Fig. 3b, Fig. S4a); $S_{TR\text{-}VPD}$, however, decreased quickly on the initial days of water deficit, and continued to decrease gradually on the following days until reaching a rather stable level even when irrigation was resumed (Fig. 3c, Fig. S4b). Among the three genotypes, "HA" exhibited high $S_{TR\text{-}Rad}$ only at the WD phase and remarkedly low $S_{TR\text{-}VPD}$ particularly at the WI stage in comparison to the remaining two genotypes (Fig. 3b & c, Fig. S4), indicating that plasticity of $S_{TR\text{-}Rad}$ and $S_{TR\text{-}VPD}$ in response to the environment is important in shaping the genotypic-specific dynamic WUE patterns. Detailed daily values of $S_{TR\text{-}Rad}$ and $S_{TR\text{-}VPD}$ are listed in Table S1 and Table S2.

3.2. Estimating dynamic WUE using the WUE model

We extended the WUE model (Eq. 2) developed by Sinclair and Ghanem (2020) to incorporate FPP data for dynamic WUE estimation (Eq. 3). To ensure the reliability of the selected model, we first tested it on an existing dataset obtained from wheat using the low-throughput canopy gas exchange method (Song et al., 2016). During a 5-day period, canopy photosynthesis rate was found to peak much earlier than canopy TR before noon (Fig. S3a), which led to a higher WUE during the whole forenoon (square in Fig. S3b). The estimated WUE using Eq. 3 at half-hourly intervals (g DW /g H_2O) based on dry matter, relying on canopy TR and VPD, was able to accurately reproduce measured WUE during daytime as shown by the lines in Fig. S3, despite a notable overestimation during the period after sunset. When analyzed on a daily basis, both the measured and estimated WUE ($WUE_{e,d}$) showed daily fluctuations (as illustrated by the triangles in Fig. S3). Nonetheless, their high consistency was evident, as demonstrated by the low RMSE of 0.00137 g g^{-1} (Fig. S3). These results validate the suitability of the WUE model utilized for estimating dynamic WUE.

Using the high-throughput FPP data obtained from Plantarray, we calculated the $WUE_{e,d}$ based on Eq.3, which showed fluctuations throughout the course of the experiment and varied significantly across genotypes (Fig. 4a, with a similar trend observed during the spring growth season as shown in Fig. S5). During the WI phase, WUE based on fresh weight (g FW /g H_2O) within this period could be measured based on traditional method, i.e., accumulated *E* dividing by accumulated biomass gain. The measured WUE returned similar result of genetic difference to $WUE_{e,d}$ based on dry weight (Fig. 4b). Among the three genotypes, "HA" possessed the highest WUE across all phases, in particular late WD stage, followed by "JC5″ and "PI296341-FR" (Fig. 4a, Fig. S5). This is in accord with the empirical knowledge that wild varieties tend to possess a higher level of drought resistance by sacrificing more biomass production (Kawasaki et al., 2000).

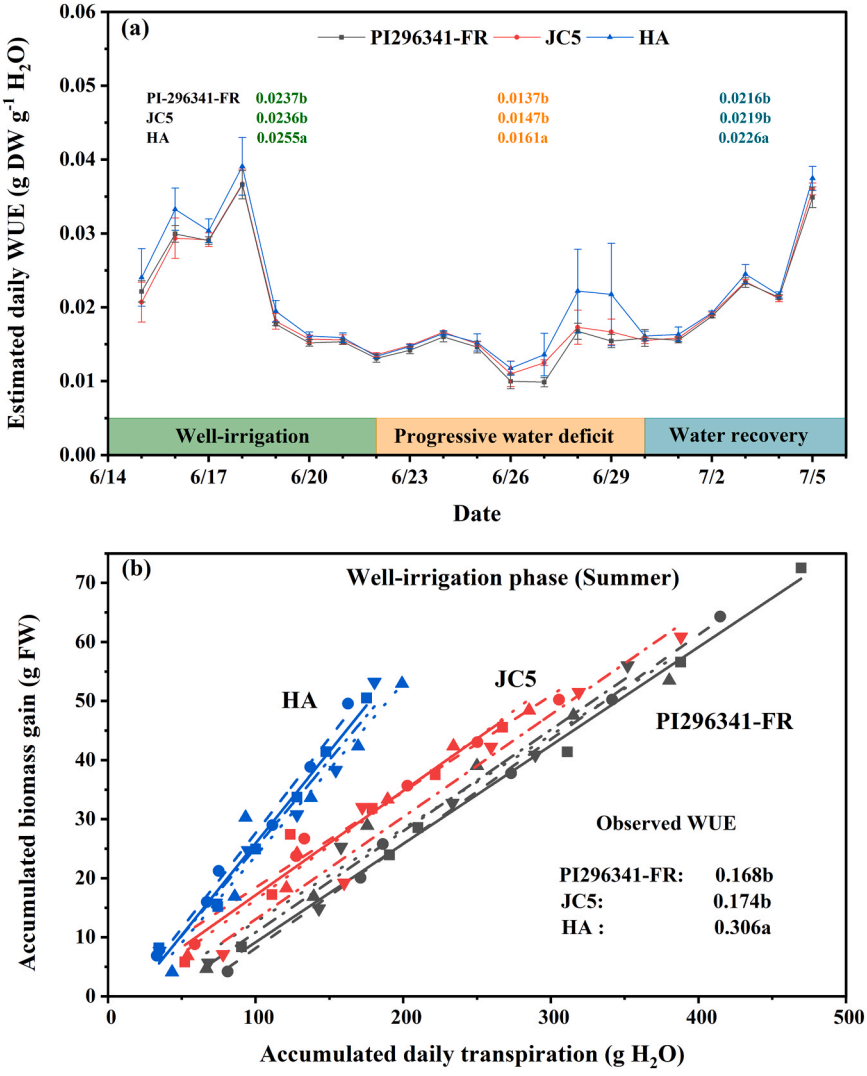

Fig. 4. Estimated daily water use efficiency ($WUE_{e,d}$) across all phases (a) and measured WUE during well-irrigation phase (b). a, $WUE_{e,d}$ (g DW g^{-1} H_2O) were calculated by Eqs. (2)–(3) with the input of continuously recorded transpiration rate and VPD by Plantarray during the summer-season experiment in 2021. Multiple comparison results among three genotypes were shown as mean values with lowercase letters to show statistically significant differences for the well-irrigation (WI), progressive water deficit (WD) and water recovery (WR) phases, respectively. b, measured WUE (g FW g^{-1} H_2O) based on accumulated biomass and transpiration during the summer-season experiment in 2021. Accumulated biomass (g FW) and transpiration (g H_2O) were calculated according to daily biomass gain and daily transpiration measured by Plantarray system during WI phase. Accumulated biomass of PI296341-FR, JC5 and HA were fitted to a linear function of accumulated transpiration for individual experiment units, and multiple comparison results among three genotypes were shown.

3.3. Transpiration ideotype design based on $S_{TR\text{-}Rad}$ and $S_{TR\text{-}VPD}$

The aforementioned results showed that watermelons with different genetic backgrounds exhibited significant variations in $S_{TR\text{-}Rad}$, $S_{TR\text{-}VPD}$, and WUE. These variations could potentially lead to differences in biomass production during the growing season. To quantitatively explore the interplays between $S_{TR\text{-}Rad}$, $S_{TR\text{-}VPD}$, TR, WUE, and their final effect on biomass production, we conducted a series of scenario simulations by combining the TR and WUE models. We conducted simulations with the inputs of 5-day meteorological data from each of the WI and WD phases (Fig. 5a, c) and the artificial combinations of $S_{TR\text{-}Rad}$ and $S_{TR\text{-}VPD}$ extremes (i.e., highest $S_{TR\text{-}Rad}$× lowest $S_{TR\text{-}VPD}$, lowest $S_{TR\text{-}Rad}$ × lowest $S_{TR\text{-}VPD}$, highest $S_{TR\text{-}Rad}$ × highest $S_{TR\text{-}VPD}$, and lowest $S_{TR\text{-}Rad}$ × highest $S_{TR\text{-}VPD}$) adopted from the 3 watermelon genotypes averaged over each 5-day course (Fig. 5b, d), where LAI was fixed to 3 to maintain a fair canopy size. Since Rad peaked much earlier than VPD in the morning (Fig. 5a, c), high $S_{TR\text{-}Rad}$ and low $S_{TR\text{-}VPD}$ was found to result in high TR during the low VPD intervals within a day and consequently a low integrated value of daily VPD weighted by TR (Eq. 1), leading to high WUE (red line in Fig. 5b, d).

Further, the estimated biomass production of different combinations was shown in Fig. 5b, d. During the WI phase, highest $S_{TR\text{-}Rad}$ × highest $S_{TR\text{-}VPD}$ and lowest $S_{TR\text{-}Rad}$ × highest $S_{TR\text{-}VPD}$ both resulted in much larger TR, which produced approximately double the biomass gain compared to the remaining combinations despite their lower WUE (Fig. 5b). While during the WD phase, the highest $S_{TR\text{-}Rad}$ × highest $S_{TR\text{-}VPD}$ still obtained the highest biomass gain benefitting from the highest TR (blue line in Fig. 5d), but the highest $S_{TR\text{-}Rad}$ × lowest $S_{TR\text{-}VPD}$ obtained a second highest biomass gain.

4. Discussion

4.1. The suitability of the selected TR model and the WUE model

There are currently numerous models available for quantifying the relationship between TR and the environment. One widely used model is the Penman-Monteith equation, which takes into account multiple environmental factors such as temperature, humidity, wind speed, and solar radiation, as well as plant characteristics such as leaf area and stomatal conductance (Zerihun et al., 2023). Other models include the Jarvis model (Jarvis et al., 1997; Wang et al., 2020), which highlights the role of stomatal conductance in regulating TR, and the Ball-Berry

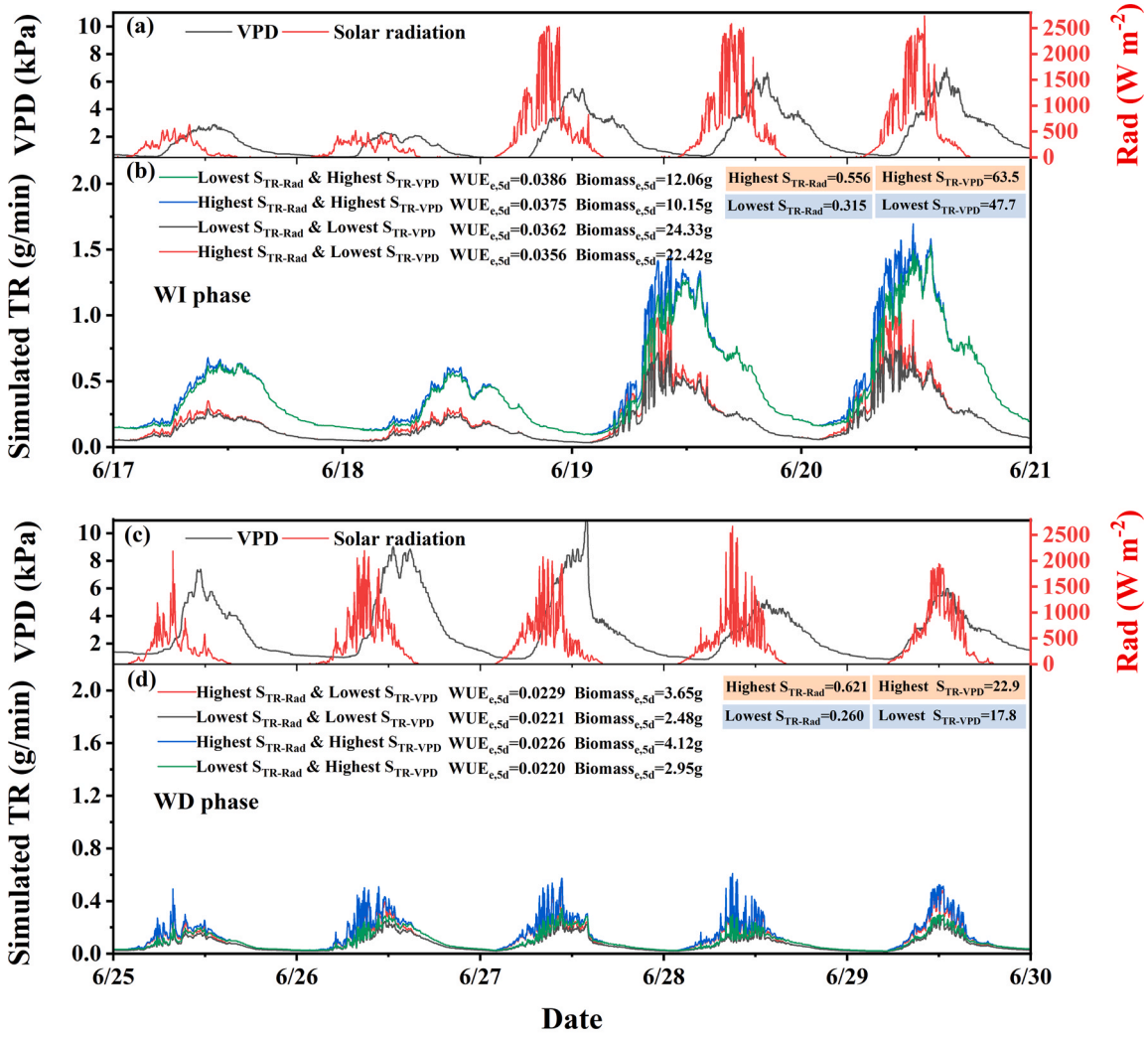

Fig. 5. Diurnal variation of solar radiation (Rad) and vapor pressure deficit (VPD), and the responsive patterns of simulated transpiration (TR) to different combinations of parameter $S_{TR\text{-}Rad}$ and $S_{TR\text{-}VPD}$. a, c five-day Rad and VPD (normalized to 0–1 scale) recorded at 3-min intervals, which were selected from the well-irrigation (WI, 6.17–6.21, a) and progressive water deficit (WD, 6.25–6.29, c) phase, respectively. The LAI was set to a constant of 3 for all simulations. Mean values of $S_{TR\text{-}Rad}$ and $S_{TR\text{-}VPD}$ for different genotypes (PI296341-FR, JC5, and HA) were calculated over each 5-day course, and the maxima and minima generated from the four combinations for simulations were shown. Mean estimated WUE and biomass gain over 5-day course were denoted as $WUE_{e,5d}$ and $Biomass_{e,5d}$, respectively.

model, which considers the relationship between stomatal conductance and atmospheric CO_2 concentration, as well as the internal resistance to CO_2 transport within the plant (Ball et al., 1987; Liu et al., 2019). In this study we ultimately chose a modified Penman-Monteith model (Jo et al., 2021; Medrano et al., 2005), as it simplifies the Penman-Monteith equation and has been successfully used in simulating TR in greenhouse crops such as cucumber and tomato. The model's input parameters are limited to Rad and VPD, which are the main environmental factors in stable greenhouse environments. Moreover, the effect of developing plant canopy on TR are incorporated in the model by simulating dynamic LAI, which makes it particularly useful for dynamic phenotyping studies.

However, accurately characterizing LAI still remains a challenge. In previous TR models, LAI was typically estimated as a function of thermal time (Wang et al., 2017) or days after transplant (Choi et al., 2020; Jo et al., 2021; Medrano et al., 2005), and often exhibited an S-shaped curve with plant growth and development. However, such approch was inadequate for our study, because the LAI of individual plants varied significantly, which could affect the parameterization of $S_{TR\text{-}Rad}$ and $S_{TR\text{-}VPD}$. In this study, we corrected the dynamic LAI by relating it to E in FPP, which fully considers the differences in dry matter accumulation and canopy development caused by E of individual plants. This method significantly improved the accuracy of the estimation of $S_{TR\text{-}Rad}$ and $S_{TR\text{-}VPD}$.

$S_{TR\text{-}Rad}$ and $S_{TR\text{-}VPD}$ were considered constant parameters throughout the growing season in some previous studies (Jo et al., 2021; Shin et al., 2014), despite the fact that they are dynamic parameters across a season or even a day under varying moisture conditions (Choi et al., 2020; Ranawana et al., 2021). Now that we have established the quantification method for these traits based on continuous physiological data, an implementation of these dynamic parameters becomes not only feasible but favorable. In this study, the treatment of $S_{TR\text{-}Rad}$ and $S_{TR\text{-}VPD}$ as dynamic parameters that change daily in response to environmental and soil conditions outperforms the fixed-parameter approach, enabling more precise quantification to help uncover the plasticity of the phenotypic traits. Using dynamic TR and VPD, the WUE model proposed by Sinclair was employed to estimate daily WUE and dry matter production, which was validated by low-throughput canopy gas exchange parameters. Compared to the expensive and low-throughput gas exchange methods used to measure WUE and photosynthesis, estimating dynamic WUE and biomass production through modeling based on lysimeter system has the advantages of being high-throughput, high--resolution, and cost-effective. The method of accurately estimating dynamic WUE based on TR and environmental VPD provides an effective way to screen WUE trait and its responsiveness to the changing environment in large germplasm resources of plants.

4.2. Influence of diurnal variation of TR on WUE and biomass production

In this research, we revealed that different genotypes of plants exhibit distinct $S_{TR\text{-}Rad}$ and $S_{TR\text{-}VPD}$, which affect the daily variation in TR and subsequently alter the WUE and biomass production. To better illustrate this impact, we conducted an additional simulation by artificially shifting the daily TR pattern forward by 1 h, in order to explore the potential impact of altered TR (Fig. S6). The daily WUE_e and $Biomass_e$ could increase by 29.9% and 20.0%, in which the enhancing WUE during the early morning contributed greatly to the biomass gain (Fig. S6). The interpretation of this result is straightforward: without sacrificing daily accumulative TR, more TR in the low-VPD morning time decreases the integral value of daily VPD weighted by TR, thus contributing to the increase of whole-day WUE and biomass gain. Such relatively small, daily improvement will accumulatively lead to an improved seasonal yield. Therefore, the pattern of diurnal TR, even under the same daily cumulative TR conditions, is considered to reverse daily WUE.

It is worth noting that there was a contrasting trend between $S_{TR\text{-}Rad}$ and $S_{TR\text{-}VPD}$ during the rehydration stage. While $S_{TR\text{-}Rad}$ showed a rapid recovery, $S_{TR\text{-}VPD}$ remained low (Fig. 3). This phenomenon could be attributed to biological reasons that the cellular machineries responsible for light response may be repaired more rapidly that those responding to VPD following water resumption. Alternatively, it may be an adaptive trait that aids in achieving an optimized daily pattern of WUE after water recovery. During the morning hours with high WUE, levels of Rad rise rapidly, while VPD levels increase during the low WUE hours near noon. The combination of recovered $S_{TR\text{-}Rad}$ and low $S_{TR\text{-}VPD}$ can result in high TR in the morning and a slower increase in TR after noon, leading to improved WUE throughout the day. However, since our experiments concluded within 5 days of water recovery, further research is needed to determine whether $S_{TR\text{-}VPD}$ can recover after longer periods of rehydration.

4.3. Proposed principle for transpiration ideotype design

Previous studies have suggested that TR exhibits a genetic foundation when exposed to naturally fluctuating conditions. However, as TR is influenced by changes in temperature, PAR, and evaporative demand, it is challenging to isolate the genetic basis of its response to individual factors (Tamang et al., 2022). The quantification of $S_{TR\text{-}Rad}$ and $S_{TR\text{-}VPD}$ offers a solution to comprehend how plants adapt to fluctuations in environmental Rad and VPD under complex circumstances. VPD plays a crucial role in driving transpiration, a process by which water is lost from plant tissues through the stomata. The genetic variation in $S_{TR\text{-}VPD}$ can be attributed to factors such as stomatal density and distribution, stomatal aperture and conductance, aquaporins and root traits (Carins Murphy et al., 2014; Ding et al., 2022; McAdam et al., 2016; Ranawana et al., 2021). Compared to $S_{TR\text{-}VPD}$, $S_{TR\text{-}Rad}$ has been relatively understudied. However, there is evidence that Rad affects the whole-plant stomatal conductance (Geetika et al., 2019), and this influence is likely mediated by the energy content of the absorbed radiation that impact the control of transpiration by stomata (Mott et al., 2011; Pieruschka et al., 2010). By combining TR and WUE model, we put forward the following principles for TR ideotype design with the combination of $S_{TR\text{-}Rad}$ and $S_{TR\text{-}VPD}$ from our experiments: in the well-irrigated agricultural areas, crop genotypes with high $S_{TR\text{-}Rad}$ and high $S_{TR\text{-}VPD}$ is favorable by producing superior yield; in the arid agricultural areas where water-saving is a necessity, genotypes with high $S_{TR\text{-}Rad}$ and low $S_{TR\text{-}VPD}$ is desired for its marvelously reduced TR yet still considerable yield; in the intermittent drought-prone areas where irrigation and water shortage alternate, genotypes showing strong plasticity in $S_{TR\text{-}Rad}$ and $S_{TR\text{-}VPD}$ that are suited to the optimized balance of yield and water consumption will be desired. Although in previous studies high-WUE crops selected by carbon isotope discrimination generally failed to match the demand of luxuriant growth (Blum, 2005, 2009), the high-WUE trait is not necessarily linked to growth limitation (Marguerit et al., 2014), which lays the foundation for synergistic improvement of WUE and yield. The FPP-enabled phenotypic selection can assist in identifying elite individuals from vast germplasm lines, specifically those with substantially high $S_{TR\text{-}Rad}$ value under both well-watered and water-scarce conditions.

4.4. Limitation clarification

It is worth noting that this study was conducted under greenhouse conditions with plants grown in medium-sized pots. A considerable difference between the environments of our experiment and the field condition exists, and the growth of plant roots may be restricted under pod cultivation. Hence, cautions should be made to extend our results to field conditions and further validations of the phenotypes will be necessary before applying them in large scale.

Furthermore, we have observed an overestimation of hourly WUE after sunset and during overcast conditions (Fig. S3). This may be attributed to the compromised reliability of K_d values under low VPD

conditions. The parameter K_d, which was originally defined by Sinclair et al. (1984), is generally known to be only species-depend (Fletcher et al., 2007). In our study, we have also incorporated K_d as a fixed parameter to estimate WUE. Although this does not affect the estimation of daily-scale WUE, there is scope for enhancing the WUE model used in this study to better accommodate low VPD conditions in the future.

5. Conclusion

In this study, we have developed a method to estimate the sensitivity of transpiration to Rad and VPD. Additionally, we have shown that it is possible to estimate daily to hourly or even instantaneous WUE by combining existing WUE models with dynamically recorded TR and VPD data from high-throughput FPP. Our findings indicate that daily WUE is influenced by the diurnal TR pattern of a plant, which is closely linked to the genotype-specific sensitivity of TR to Rad and VPD. Our proposal to increase WUE involves reducing $S_{TR\text{-}VPD}$ while compensating for its negative impact on TR by increasing $S_{TR\text{-}Rad}$.

CRediT authorship contribution statement

Ting Sun: Investigation, Writing – original draft, Software. **Rui Cheng:** Resources, Validation. **Rujia Jiang:** Formal analysis, Visualization, Software. **Pei Xu:** Writing – review & editing, Project administration, Funding acquisition. **Other authors:** Formal analysis, Data curation.

Declaration of Competing Interest

The authors declare that they have no known competing financial interests or personal relationships that could have appeared to influence the work reported in this paper.

Data Availability

No data was used for the research described in the article.

Acknowledgments

We thank the supports of National Key Research & Development Program of China (2022YFE0198000), the Research & Development Program of Ningbo (2021Z006) and the Key Scientific and Technological Grant of Zhejiang for Breeding New Agricultural Varieties (2021C02066–5, 2021C02067–7). We express our gratitude to the National Engineering and Technology Center for Information Agriculture at Nanjing Agricultural University for providing us with the CATPS datasets.

Appendix A. Supporting information

Supplementary data associated with this article can be found in the online version at doi:10.1016/j.eja.2023.126955.

References

Ball, J.T., Woodrow, I.E., Berry, J.A., 1987. A model predicting stomatal conductance and its contribution to the control of photosynthesis under different environmental conditions. In: Biggins, J. (Ed.), Progress in Photosynthesis Research: Volume 4 Proceedings of the VIIth International Congress on Photosynthesis Providence. Springer Netherlands, Dordrecht, pp. 221–224.

Blum, A., 2005. Drought resistance, water-use efficiency, and yield potential-are they compatible, dissonant, or mutually exclusive. Aust. J. Agric. Res. 56 (11), 1159–1168. https://doi.org/10.1071/ar05069.

Blum, A., 2009. Effective use of water (EUW) and not water-use efficiency (WUE) is the target of crop yield improvement under drought stress. Field Crops Res. 112 (2–3), 119–123. https://doi.org/10.1016/j.fcr.2009.03.009.

Carins Murphy, M.R., Jordan, G.J., Brodribb, T.J., 2014. Acclimation to humidity modifies the link between leaf size and the density of veins and stomata. Plant Cell Environ. 37 (1), 124–131. https://doi.org/10.1111/pce.12136.

Chenu, K., Van Oosterom, E.J., McLean, G., Deifel, K.S., Fletcher, A., Geetika, G., Tirfessa, A., Mace, E.S., Jordan, D.R., Sulman, R., Hammer, G.L., 2018. Integrating modelling and phenotyping approaches to identify and screen complex traits: transpiration efficiency in cereals. J. Exp. Bot. 69 (13), 3181–3194. https://doi.org/10.1093/jxb/ery059.

Choi, Y.B., Shin, J.H., 2020. Development of a transpiration model for precise irrigation control in tomato cultivation. Sci. Hortic. 267, 109358 https://doi.org/10.1016/j.scienta.2020.109358.

Dalal, A., Bourstein, R., Haish, N., Shenhar, I., Wallach, R., Moshelion, M., 2019. Dynamic physiological phenotyping of drought-stressed pepper plants treated with "productivity-enhancing" and "survivability-enhancing" biostimulants. Front. Plant Sci. 10, 00905. https://doi.org/10.3389/fpls.2019.00905.

Dalal, A., Shenhar, I., Bourstein, R., Mayo, A., Grunwald, Y., Averbuch, N., Attia, Z., Wallach, R., Moshelion, M., 2020. A telemetric, gravimetric platform for real-time physiological phenotyping of plant-environment interactions. J. Vis. Exp. 162, 1–28. https://doi.org/10.3791/61280.

Ding, L., Milhiet, T., Parent, B., Meziane, A., Tardieu, F., Chaumont, F., 2022. The plasma membrane aquaporin ZmPIP2;5 enhances the sensitivity of stomatal closure to water deficit. Plant, Cell Environ. 45 (4), 1146–1156. https://doi.org/10.1111/pce.14276.

Fletcher, A.L., Sinclair, T.R., Allen, L.H., 2007. Transpiration responses to vapor pressure deficit in well watered 'slow-wilting' and commercial soybean. Environ. Exp. Bot. 61, 145–151.

Fracasso, A., Magnanini, E., Marocco, A., Amaducci, S., 2017. Real-time determination of photosynthesis, transpiration, water-use efficiency and gene expression of two *Sorghum bicolor* (Moench) genotypes subjected to dry-down. Front. Plant Sci. 8, 00932. https://doi.org/10.3389/fpls.2017.00932.

Geetika, G., van Oosterom, E.J., George-Jaeggli, B., Mortlock, M.Y., Deifel, K.S., McLean, G., Hammer, G.L., 2019. Genotypic variation in whole-plant transpiration efficiency in sorghum only partly aligns with variation in stomatal conductance. Funct. Plant Biol. 46 (12), 1072–1089. https://doi.org/10.1071/FP18177.

Génard, M., Memmah, M.-M., Quilot-Turion, B., Vercambre, G., Baldazzi, V., Le Bot, J., Bertin, N., Gautier, H., Lescourret, F., Pagès, L., 2016. Process-based simulation models are essential tools for virtual profiling and design of ideotypes: example of fruit and root. Crop Syst. Biol. 83–104.

Ghanem, M.E., Kehel, Z., Marrou, H., Sinclair, T.R., 2020. Seasonal and climatic variation of weighted VPD for transpiration estimation. Eur. J. Agron. 113, 125966 https://doi.org/10.1016/j.eja.2019.125966.

Gosa, S.C., Lupo, Y., Moshelion, M., 2019. Quantitative and comparative analysis of whole-plant performance for functional physiological traits phenotyping: new tools to support pre-breeding and plant stress physiology studies. Plant Sci. (Amst., Neth.) 282, 49–59. https://doi.org/10.1016/j.plantsci.2018.05.008.

Halperin, O., Gebremedhin, A., Wallach, R., Moshelion, M., 2017. High-throughput physiological phenotyping and screening system for the characterization of plant-environment interactions. Plant J. 89 (4), 839–850. https://doi.org/10.1111/tpj.13425.

IPCC, 2021. Climate change 2021: the physical science basis. Contribution of working group I to the sixth assessment report of the intergovernmental panel on climate change. Cambridge, United Kingdom and New York. Cambridge University Press, NY, USA.

Jarvis, P.G., Monteith, J.L., Weatherley, P.E., 1997. The interpretation of the variations in leaf water potential and stomatal conductance found in canopies in the field. Philos. Trans. R. Soc. Lond. B, Biol. Sci. 273 (927), 593–610. https://doi.org/10.1098/rstb.1976.0035.

Jhou, H.C., Wang, Y.N., Wu, C.S., Yu, J.C., Chen, C.I., 2017. Photosynthetic gas exchange responses of *Swietenia macrophylla* King and *Melia azedarach* L. plantations under drought conditions. Bot. Stud. 58 (1), 57. https://doi.org/10.1186/s40529-017-0212-8.

Jo, W.J., Shin, J.H., 2021. Development of a transpiration model for precise tomato (*Solanum lycopersicum* L.) irrigation control under various environmental conditions in greenhouse. Plant Physiol. Biochem. 162, 388–394. https://doi.org/10.1016/j.plaphy.2021.03.005.

Katsoulas, N., Stanghellini, C., 2019. Modelling crop transpiration in greenhouses: different models for different applications. Agronomy 9 (7), 392. https://doi.org/10.3390/agronomy9070392.

Kawasaki, S., Miyake, C., Kohchi, T., Fujii, S., Uchida, M., Yokota, A., 2000. Responses of wild watermelon to drought stress: accumulation of an ArgE homologue and citrulline in leaves during water deficits. Plant Cell Physiol. 41 (7), 864–873. https://doi.org/10.1093/pcp/pcd005.

Kubota, C., 2020. Growth, Development, Transpiration, and Translocation as Affected by Abiotic Environmental Factors. In: Kozai, T., Niu, G., Takagaki, M. (Eds.), Plant factory, second ed. Academic Press, pp. 207–220.

Li, Y., Wu, X., Xu, W., Sun, Y., Wang, Y., Li, G., Xu, P., 2020. High-throughput physiology-based stress response phenotyping: advantages, applications and prospective in horticultural plants. Hortic. Plant J. 7 (3), 181–187. https://doi.org/10.1016/j.hpj.2020.09.004.

Liu, N., Wang, H., He, X., Deng, Z., Zhang, C., Zhang, X., Guan, H., 2019. A hybrid transpiration model for water-limited conditions. J. Hydrol. 578. https://doi.org/10.1016/j.jhydrol.2019.124104.

Marguerit, E., Bouffier, L., Chancerel, E., Costa, P., Lagane, F., Guehl, J.M., Plomion, C., Brendel, O., 2014. The genetics of water-use efficiency and its relation to growth in maritime pine. J. Exp. Bot. 65 (17), 4757–4768. https://doi.org/10.1093/jxb/eru226.

McAdam, S.A., Sussmilch, F.C., Brodribb, T.J., 2016. Stomatal responses to vapour pressure deficit are regulated by high speed gene expression in angiosperms. Plant Cell Environ. 39 (3), 485–491. https://doi.org/10.1111/pce.12633.

Medrano, E., Lorenzo, P., Sánchez-Guerrero, M.C., Montero, J.I., 2005. Evaluation and modelling of greenhouse cucumber-crop transpiration under high and low radiation conditions. Sci. Hortic. 105 (2), 163–175. https://doi.org/10.1016/j.scienta.2005.01.024.

Mott, K.A., Peak, D., 2011. Alternative perspective on the control of transpiration by radiation. PNAS 108 (49), 19820–19823. https://doi.org/10.1073/pnas.1113878108.

Nelson, J.A., Carvalhais, N., Migliavacca, M., Reichstein, M., Jung, M., 2018. Water-stress-induced breakdown of carbon–water relations: indicators from diurnal FLUXNET patterns. Biogeosciences 15 (8), 2433–2447. https://doi.org/10.5194/bg-15-2433-2018.

Oogathoo, S., Houle, D., Duchesne, L., Kneeshaw, D., 2020. Vapour pressure deficit and solar radiation are the major drivers of transpiration of balsam fir and black spruce tree species in humid boreal regions, even during a short-term drought. Agric. For. Meteorol. 291, 108063 https://doi.org/10.1016/j.agrformet.2020.108063.

Peddinti, S.R., Kambhammettu, B.V.P., Rodda, S.R., Thumaty, K.C., Suradhaniwar, S., 2019. Dynamics of ecosystem water use efficiency in citrus orchards of central India using eddy covariance and landsat measurements. Ecosystems 23 (3), 511–528. https://doi.org/10.1007/s10021-019-00416-3.

Pieruschka, R., Huber, G., Berry, J.A., 2010. Control of transpiration by radiation. PNAS 107 (30), 13372–13377. https://doi.org/10.1073/pnas.0913177107.

Ranawana, S., Siddique, K.H.M., Palta, J.A., Stefanova, K., Bramley, H., 2021. Stomata coordinate with plant hydraulics to regulate transpiration response to vapour pressure deficit in wheat. Funct. Plant Biol. 48 (9), 839–850. https://doi.org/10.1071/FP20392.

Shin, J.H., Park, J.S., Son, J.E., 2014. Estimating the actual transpiration rate with compensated levels of accumulated radiation for the efficient irrigation of soilless cultures of paprika plants. Agric. Water Manag. 135, 9–18. https://doi.org/10.1016/j.agwat.2013.12.009.

Sinclair, T.R., Vadez, V., 2012. The future of grain legumes in cropping systems. Crop Pasture Sci. 63.

Sinclair, T.R., Ghanem, M.E., 2020. Plant-based predictions of canopy transpiration instead of meteorological approximations. Crop Sci. 60, 1133–1141. https://doi.org/10.1002/csc2.20067.

Sinclair, T.R., Tanner, C.B., Bennett, J.M., 1984. Water-use efficiency in crop production. Bioscience 1, 36–40.

Song, Q., Xiao, H., Xiao, X., Zhu, X.-G., 2016. A new canopy photosynthesis and transpiration measurement system (CAPTS) for canopy gas exchange research. Agric. For. Meteorol. 217, 101–107. https://doi.org/10.1016/j.agrformet.2015.11.020.

Song, Q.H., Fei, X.H., Zhang, Y.P., Sha, L.Q., Liu, Y.T., Zhou, W.J., Wu, C.S., Lu, Z.Y., Luo, K., Gao, J.B., Liu, Y.H., 2017. Water use efficiency in a primary subtropical evergreen forest in Southwest China. Sci. Rep. 7, 43031. https://doi.org/10.1038/srep43031.

Steduto, P., Hsiao, T.C., Fereres, E., Raes, D., 2012. Crop Yield Response to Water. FAO, Rome.

Tamang, B.G., Monnens, D., Anderson, J.A., Steffenson, B.J., Sadok, W., 2022. The genetic basis of transpiration sensitivity to vapor pressure deficit in wheat. Physiol. Plant. 174 (5), e13752 https://doi.org/10.1111/ppl.13752.

Tanner, C.B., Sinclair, T.R., 1983. Efficient water use in crop production: research or research? In Limitations to Efficient Water Use in Crop Production, pp. 1-27.

Vadez, V., Kholova, J., Medina, S., Kakkera, A., Anderberg, H., 2014. Transpiration efficiency: new insights into an old story. J. Exp. Bot. 65 (21), 6141–6153. https://doi.org/10.1093/jxb/eru040.

Wang, H., Sánchez-Molina, J.A., Li, M., Berenguel, M., Yang, X.T., Bienvenido, J.F., 2017. Leaf area index estimation for a greenhouse transpiration model using external climate conditions based on genetics algorithms, back-propagation neural networks and nonlinear autoregressive exogenous models. Agric. Water Manag. 183, 107–115. https://doi.org/10.1016/j.agwat.2016.11.021.

Wang, H., Guan, H., Liu, N., Soulsby, C., Tetzlaff, D., Zhang, X., 2020. Improving the Jarvis-type model with modified temperature and radiation functions for sap flow simulations. J. Hydrol. 587. https://doi.org/10.1016/j.jhydrol.2020.124981.

Xu, P., Moshelion, M., Wu, X., Halperin, O., Wang, B., Luo, J., Wallach, R., Wu, X., Lu, Z., Li, G., 2015. Natural variation and gene regulatory basis for the responses of asparagus beans to soil drought. Front. Plant Sci. 6 (3), 891. https://doi.org/10.3389/fpls.2015.00891.

Yang, Y.J., Bi, M.H., Nie, Z.F., Jiang, H., Liu, X.D., Fang, X.W., Brodribb, T.J., 2021. Evolution of stomatal closure to optimize water-use efficiency in response to dehydration in ferns and seed plants. N. Phytol. 230 (5), 2001–2010. https://doi.org/10.1111/nph.17278.

Yu, G., Zhuang, J., Zhen, Liang, 2001. An attempt to establish a synthetic model of photosynthesis-transpiration based on stomatal behavior for maize and soybean plants grown in field. J. Plant Physiol. 158 (7), 861–874. https://doi.org/10.1078/0176-1617-00177.

Yu, G.R., Wang, Q.F., Zhuang, J., 2004. Modeling the water use efficiency of soybean and maize plants under environmental stresses: application of a synthetic model of photosynthesis-transpiration based on stomatal behavior. J. Plant Physiol. 161 (3), 303–318. https://doi.org/10.1078/0176-1617-00972.

Zerihun, D., Sanchez, C.A., French, A.N., 2023. Derivation of the Penman–Monteith equation with the thermodynamic approach. I: a review and theoretical development. J. Irrig. Drain. Eng. 149 (5), 04023007 https://doi.org/10.1061/JIDEDH.IRENG-9887.